



Sensors grid influence on damage detection for masonry towers.

A numerical investigation based on the modal curvatures

Gianni Bartoli^a, Michele Betti^a, Barbara Pintucchi^a, Giacomo Zini^a

^a *Dipartimento di Ingegneria Civile e Ambientale, Via di Santa Marta 3, 50139 Firenze*

Keywords: Modal curvature, Sensors grid, Masonry towers, Damage detection, Numerical models

ABSTRACT

This paper aims at contributing to verify the effectiveness of a dynamic monitoring system for early damage detection with reference to slender masonry towers. In the first part, a reference scheme of tower constrained by adjacent buildings is numerically analyzed: changes in the main modal parameters - natural frequencies, mode shapes and modal curvatures - are evaluated. Subsequently, the numerical results are employed to investigate the precision level needed to identify the damage in terms of spatial resolution. Lastly, a local approach based on strain measurements is investigated.

1 INTRODUCTION

To assess existing buildings health status and to detect possible ongoing damage processes, vibration-based structural monitoring is increasingly applied (Ceravolo *et al.* 2016; Pierdicca *et al.* 2016). This method appears to be attractive especially for historic structures such as masonry towers that, by nature, are easily susceptible to ambient vibrations (wind, traffic, swinging of bells, earthquakes, etc.). This is testified by the growing number of long-term monitoring activities on masonry towers, bell towers and other masonry structures prone to damage (Gentile *et al.* 2016; Ubertini *et al.* 2017; Cavalagli *et al.* 2018).

Due to its low invasiveness and low cost together with the conceptual clarity of the approach (the occurrence of damage results in a change of the modal characteristic of the structure), damage detection techniques using dynamic measurements have become an appealing strategy and a very popular approach successfully applied in the last decades to various

structural typologies (Sohn *et al.* 2003; Morassi and Vestroni 2008; Ramos *et al.* 2010; Facchini *et al.* 2014; Betti *et al.* 2015; Frigui *et al.* 2018).

To date, some consistent conclusions on the sensitiveness to damage of some modal parameters have been provided (Pandey *et al.* 1991; Agarwal and Chaudhuri 2015) and some reliable methodologies and procedure have been proposed and verified (Salawu 1997; Chang *et al.* 2003) for reinforced and/or prestressed concrete or steel structures. On the contrary, with respect to historic masonry buildings, still a number of issues remains opened, namely: i) the high sensitiveness of the modal properties to the environmental conditions; ii) the possibility to properly detect the irreversible variation of the dynamic characteristics due to occurred or incipient damage phenomena, iii) the level of refinement of the sensors grid able to identify the damage (both in terms of sensors sensitivity and sensors spatial resolution), and iv) the identification of a modal parameter, an ensembles and/or a combinations of them, that can actually indicate the presence of a damage process.

Starting from the pioneering studies of (Pandey *et al.* 1991) on a simple numerical



model, among the various modal parameters, the modal curvature appears to be one of the most sensitive parameters to damage. With respect to masonry towers, it has been demonstrated in previous studies (Bartoli *et al.* 2017a,b) that: i) due to the typology of damage, the damage mainly affect the first frequency and changes are up to about 2.5% with respect to the undamaged value; ii) modal shapes are less sensitive to damage, as the damage introduces localized variations; iii) indexes like MAC (Modal Assurance Criterion) and MTMAC (Modified Total MAC) are not able to identify differences between the undamaged and the damaged configuration; on the contrary damage indexes like MS and MSCS (Rucevskis and Wesolowski 2010), computing the absolute difference between the mode shapes of the undamaged and the damaged structure, seems able to assess the location of the damage.

Assuming that the modal curvatures are the most sensitive modal parameter to damage, this paper investigates the influence of the sensors grid on damage detection for masonry towers. In the first part of the paper a numerical model of a representative masonry tower is introduced. The numerical model is employed to perform non-linear time-history analyses under the action of real earthquakes. The aim is to numerically represent realistic damage scenarios that can occur in real structures due to earthquakes. The numerical results are subsequently assumed as reference and are employed in the second part of the paper to evaluate the influence of the sensors grid. The use of numerical results as reference results has a twofold purpose: i) it is possible to simulate a wide range of both damaged and undamaged configuration; ii) it is possible to assume both refined and course sensors grid (each node of the numerical model is assumed as a possible position of the sensors) and consequently quantify the needed refinement of the sensor grid on the damage detection.

In particular, based on the data usually available in an experimental test, it is assumed that only mode shapes and frequencies are available.

The aim of the paper is hence to give a contribution in understanding the suitability of possible methodology to obtain damage indicators based on modal curvatures.

2 REFERENCE TOWER AND MODELLING DESCRIPTION

2.1 Scheme of the reference tower

The dimension and the typology of the prototype of the considered masonry tower have been assumed according to those of the *Torre Grossa* of San Gimignano (Siena, Italy; Bartoli *et al.* 2103).

The tower has a square cross section with an external side of about 9.5×9.5 m, with an overall height of about 55 m. Up to the height of about 20 m the tower is incorporated into an earlier building, the Town Hall.

2.2 Input ground motions

Four historically recorded accelerograms whose main characteristics are listed in Table 1, has been used as seismic inputs.

The pseudo-acceleration spectra of the selected accelerograms, for a viscous damping ratio of 5%, are given in Figure 1; peaks cover a range varying from 0.39 s to 1.06 s.

Table 1. Input ground motions used.

Cas e	Earthquake	Date	Mw	Time (s)	PGA (g)
s1	Tabas	1978	7.4	63.40	0.925
s2	Montenegro (1)	1979	6.9	47.80	0.374
s3	Northridge	1994	6.7	38.58	0.726
s4	Montenegro (2)	1979	6.9	47.80	0.362

Seismic inputs s2÷s4 have been applied unscaled, while a scale factor equal to 0.86 was employed for seismic input s1 to avoid (numerical) collapse of the tower during the analysis.

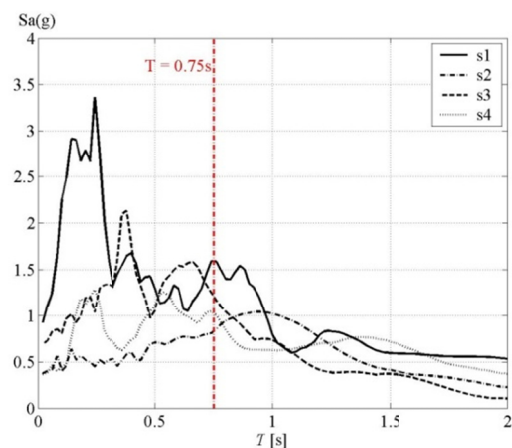


Figure 1. Pseudo-acceleration spectra of the inputs used.



2.3 Modelling approach

The analyzed masonry tower has been modelled as a continuous beam with a rectangular cross-section and mass m uniformly distributed along its length. The material's behavior is described by a nonlinear constitutive equation, which assumes masonry to have null tensile strength and a limited compressive strength (Lucchesi and Pintucchi 2007; Lucchesi *et al.* 2015). Then, a damage process after crushing is accounted for, and a linear piecewise law is used to describe the softening behavior in compression, as shown by Figure 2.

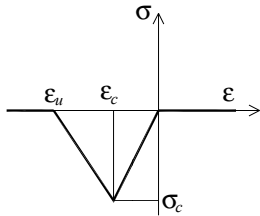


Figure 2: Masonry behaviour under uniaxial stress.

According to the assumed behavior, a damage function (Pintucchi and Zani 2016) has been determined to define the constitutive law for the beam section, where damage is represented by a reduction of the initial mechanical properties (Young modulus and compressive strength).

The numerical simulations have been conducted using an Euler-Bernoulli beam model available within the finite element code MADY (Lucchesi and Pintucchi 2007; Bartoli *et al.* 2017c), where a standard nonlocal averaging approach has been used in the damage procedure, to avoid mesh sensitivity and convergence to incorrect solutions.

A procedure for solving the eigenvalues problem at each step of a loading process has been introduced into the code. When the structure behaves elastically, the modal properties can be found through the equation:

$$K\phi_i - \omega_i^2 M\phi_i = 0 \quad (1)$$

where K and M are the global stiffness and mass matrices, ω and Φ are the angular frequency and the mode shape, and i is the number of each of the modes.

Conversely, when the structure undergoes a nonlinear behavior, i.e. cracking and/or crushing, the equation that provides the modal properties (of the nonlinear model) is:

$$\tilde{K}\tilde{\phi}_i - \tilde{\omega}_i^2 M\tilde{\phi}_i = 0 \quad (2)$$

where \tilde{K} is the tangent stiffness matrix of the structure.

It is worth noting that, due to the no-tension model used and in view of Eqs. (1) and (2), when cracking occurs under the loading process, the modal properties change with respect to the unloaded case; however, if cracks are re-closed in the final configuration, the evaluated modal properties are equal to the initial ones. Conversely, if the structure undergoes crushing and the softening branch is attained, a damage process occurs that leads to a permanent variation of the modal properties.

2.4 Numerical model

The built beam model (Figure 3) approximates the actual geometry of the *Torre Grossa*; the constraint offered by the neighbouring buildings extending for a height of about 20 m from the ground has been modelled with a set of lateral elastic restraints.

For as mechanical characteristics are concerned - Young's modulus E and mass density ρ - the values suggested in (Bartoli *et al.* 2013) have been assumed, i.e. $E = 3.0$ GPa, $\rho = 1800$ kg/m³; then, the stiffness of the lateral constraints have been chosen so as to obtain the numerical first natural periods - $T_1 = 0.75$ s - close to those evaluated on the basis of the experimental campaigns (Bartoli *et al.* 2013).

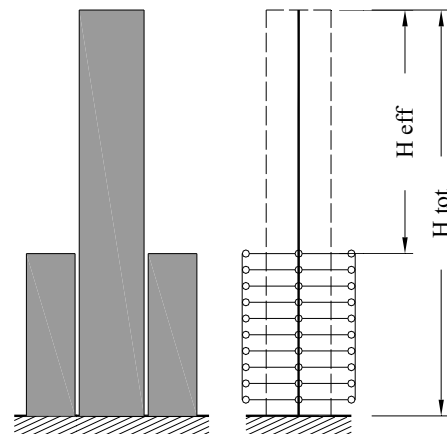


Figure 3. MADY beam model.

The limit value of the compressive deformability ϵ_u , has been chosen to have a strain ductility $\mu_\epsilon = \epsilon_u / \epsilon_c = 3$ (Figure 2). The assumed parameters are listed in Table 2.



A viscous damping coefficient of 2% for the first two flexural modes has been considered in all the dynamic analyses.

Table 2. Geometrical and mechanical parameters.

H_{tot} (m)	H_{eff} (m)	E (GPa)	σ_c (MPa)	μ_c (-)
50	20	3.0	5.0	3.0

The damage scenario obtained is the same for all the four applied accelerograms: crushing occurs in an area located around the level at which the tower rises from the adjacent buildings (Bartoli *et al.* 2017a,b).

Whilst the code allows to calculate, by using Hermite shape functions, the transverse displacements and their derivatives (required to draw mode shapes, rotations and modal curvatures), only displacement of the mode shape have been considered. They are assumed as reference values and employed in the next section to independently calculate the modal curvature and to assess the effect of the sensor grid.

3 DAMAGE INDICATORS

In a dynamic experimental test, data commonly available are frequencies and mode shapes. The modal curvatures can be derived from these data, as shown in the following.

Under the hypothesis of the Euler-Bernoulli beam theory, the second derivative of the modal displacements (ϕ) along the longitudinal axis approximates the modal curvature:

$$GMC = \frac{\phi''}{(1 + (\phi')^2)^{3/2}} \approx \phi'' \quad (3)$$

where \bullet' is the spatial derivative with respect to the beam axis. This case, where the modal curvature is evaluated directly through the second derivative of the (discrete) modal displacements, is here called Global Modal Curvature (GMC).

The curvature damage factor can be defined (Wahab and De Roeck 1999):

$$GCDF = \frac{1}{n} \sum_{i=1}^n |\phi''_{id} - \phi''_{iu}| \quad (4)$$

where ϕ''_{id} and ϕ''_{iu} are the i -th mode shape curvature of the damaged and undamaged structure and n represents the number of mode shapes considered. This index, calculated starting

from the value of the modal curvature obtained by Eq. (3), will be denoted as GCDF (Global Curvature Damage Factor).

This case aims to represent the situation in which the tower is monitored with horizontal accelerometers and the curvatures can be measured starting from the modal displacements obtained by accelerometers.

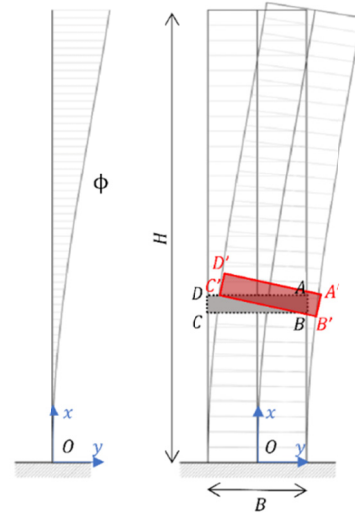


Figure 4. Scheme of the first mode shape: the deformed configuration between two measuring points A and B is drawn in red.

It is possible to consider an alternative formulation to be employed for evaluating the modal curvature, by defining it as a function of the measured strains (Figure 4). To differentiate the modal curvature evaluated from the mode shape (GMC) from the modal curvature evaluated by the measured strain, this second procedure is here called Local Modal Curvature (LMC):

$$LMC = \frac{\Delta \varepsilon}{y} \quad (5)$$

where $\Delta \varepsilon$ is the difference between the measured modal strain on a generic longitudinal fiber and the strain due to the axial force, while y denotes the distance of this fiber from the neutral axis.

Analogously to Eq. (4), the following index can be defined:

$$LCDF = \frac{1}{n} \sum_{i=1}^n LMC_i \quad (6)$$

This second case represents the situation where strain gauges are installed on a tower and the modal curvatures are locally evaluated by means of strain measurements.



4 DISCUSSION OF THE RESULTS

4.1 Changes on the main frequencies

The four seismic inputs s2÷s4 have been applied to the numerical model and the first three eigenfrequencies have been evaluated after the damaged induced by earthquake actions. The results obtained in terms of changes of the main frequencies are reported in Table 3 and Figure 5, compared with the undamaged scenario.

Table 3. Changes on the main frequencies for each damage scenario.

	f_1 (Hz)	f_2 (Hz)	f_3 (Hz)
undamaged	1.466	7.940	18.520
s1	1.445 (1.42%)	7.929 (0.14%)	18.404 (0.63%)
s2	1.458 (0.52%)	7.934 (0.08%)	18.479 (0.22%)
s3	1.466 (-)	7.940 (-)	18.520 (-)
s4	1.433 (2.27%)	7.916 (0.30%)	18.344 (0.96%)

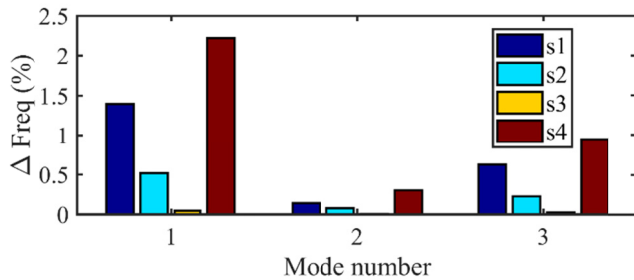


Figure 5. Main frequency variation for every damage scenario.

The maximum variation is observed on the first frequency when the seismic input s4 is applied. It is about 2.2%, a value that in real cases might be hidden by the effect of the environmental parameters.

4.2 Influence of the measurement grid spacing

To evaluate the influence of the sensor measurements grid, the case in which the results of the modal displacement in each node of the model are known (this is here denoted as y_{ref}) has been assumed as a purely theoretical reference case. This reference case is compared with other cases with a reduced number of information (denoted as y_i) which may correspond to the number of instruments available in an experimental test. It is worth noting that reducing the number of y_i obviously leads to a reduction of the resolution of the mode shapes.

Assuming a discrete grid of measurement, an analytical expression of the Global Modal Curvature (GMC) can be obtained by using the central difference method.

Assuming, as usual in an experimental investigation, a non-uniformly spaced grid of sensors, whose positions are denoted by x_i and their relative distances by $h_i = x_i - x_{i-1}$, the GMC can be obtained by a linear superposition of the values that the discrete function ϕ (i.e. the discrete displacement of the mode shape) assumes in three consecutive points [$x_{i-1}, \phi(x_{i-1}); x_i, \phi(x_i); x_{i+1}, \phi(x_{i+1})$]:

$$\phi''(x_i) = \alpha_i \phi(x_i) + \beta_i \phi(x_{i+1}) + \gamma_i \phi(x_{i-1}) \quad (7)$$

The weighting coefficients $\alpha_i, \beta_i, \gamma_i$ can be calculated from the Taylor's series of the function arrested at the second order for in the central point. By solving the Eq. (7), the following values of the coefficients $\alpha_i, \beta_i, \gamma_i$ are obtained:

$$\alpha_i = -\frac{2}{h_i h_{i+1}}$$

$$\beta_i = \frac{2}{h_{i+1}(h_i + h_{i+1})} \quad (8)$$

$$\gamma_i = \frac{2}{h_i(h_i + h_{i+1})}$$

It is worth noting that when the spatial grid is uniform ($h_i = h_{i+1} = h$), Eq. (7) reduces to the classical formula of the central difference method. If $h_i, h_{i+1} \rightarrow 0$ the discrete numerical values will reach the analytical values, minimizing the numerical errors.

Based on Eq. (7), the modal curvatures have been obtained starting from the mode shapes. Figure 6 reports the modal curvatures obtained for the undamaged configuration, whereas Figure 7 shows the analogous results for the damaged configuration obtained after the input s1.

In both cases, a different number of sensors (6, 10 and 20) has been considered to reconstruct the modal curvature; each case has been indicated as y_i . To highlight the capability of the procedure to capture the actual modal curvature and its dependence on the grid spacing, the curve y_{ref} of the reference case has been also plotted in each graph.

Figure 8 show the GCDF evaluated by using the first three modal curvatures obtained for each



seismic input used. The obtained results suggest that a significant spatial resolution is needed to assess the damage and to avoid false positives. This outcome highlights a criticism related to the great number of sensors required during an experimental investigation.

Of course, largest errors occur in positions close to the boundary of the tower rather than in those positions more close to the central part of the tower, due to the procedure used to estimate the modal curvatures.

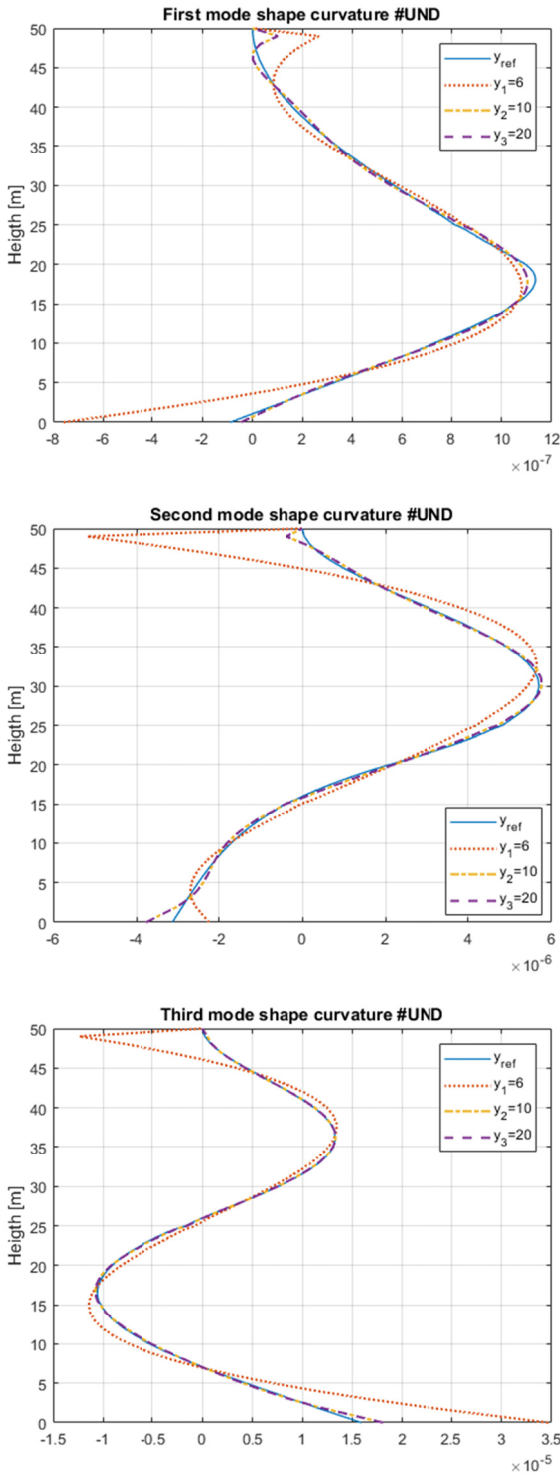


Figure 6. Undamaged configuration: modal curvatures reconstructed with various sensor grids.

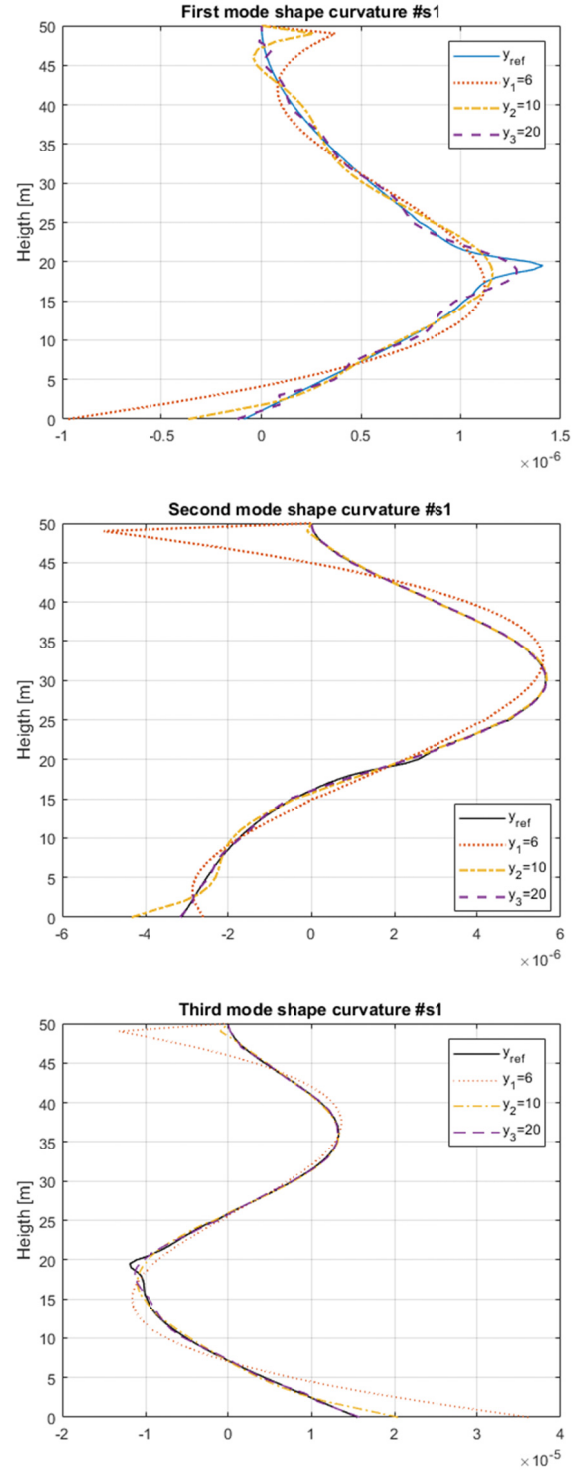


Figure 7. Damaged configuration: modal curvatures reconstructed with various sensor grids (after damage caused by seismic input s1).

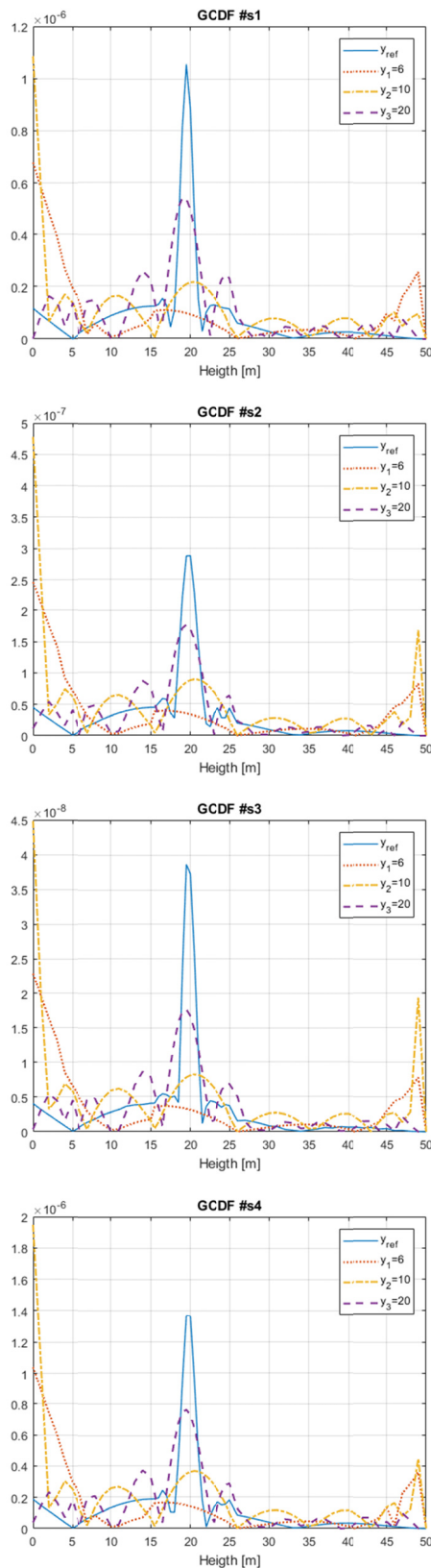


Figure 8. Sensitiveness of GCDF to the sensor grid.

4.3 Influence of the position and length for the LMC measurements

The ability of the LMC (i.e. the possibility to assess the occurrence of damage through a direct measurement of the local strain) to work as damage indicator is investigated by analyzing: a) the role of the measurement length; b) the role of the position of the sensors along the tower height.

Results are summarized in Figure 9. The bounded domain where the LCDF allows the damage detection goes from 17.5-22.5 m in terms of position and from 1-6 m in terms of reference length.

Obviously, the best identification of the damaged area are obtained when the strain measurement is centered in the damaged zone; notwithstanding, longer base lengths are capable to detect damages also if they are located – though not exactly centered – across the damaged zone.

5 CONCLUSIVE REMARKS

With reference to a simplified structural scheme of masonry tower bounded by lower adjacent buildings, some damage scenarios due to seismic actions have been numerically simulated. The numerical results have been employed as reference data to evaluate the effect of the sensor grid refinement for damage detection, and some damage indexes built starting from the modal curvatures have been numerically evaluated.

Results show that to assess damage a significant number of sensors is needed. Taking into account that large number of data are required to assure the needed refinement of the modal curvature, a procedure based on local strain measurements has also been investigated.

This method allows to avoid the numerical calculation of the modal shape curvature starting from the experimentally-evaluated mode shapes, that should require a dense measurement layout. As expected, local strain measurement is able to locate damage when the strain measurement is centered in the damaged zone. Nevertheless, it is interesting that even large reference lengths of the strain measurement seems able to locate damage.

Further studies will investigate the possibility to combine accelerometer and strain measurements for early damage detection.

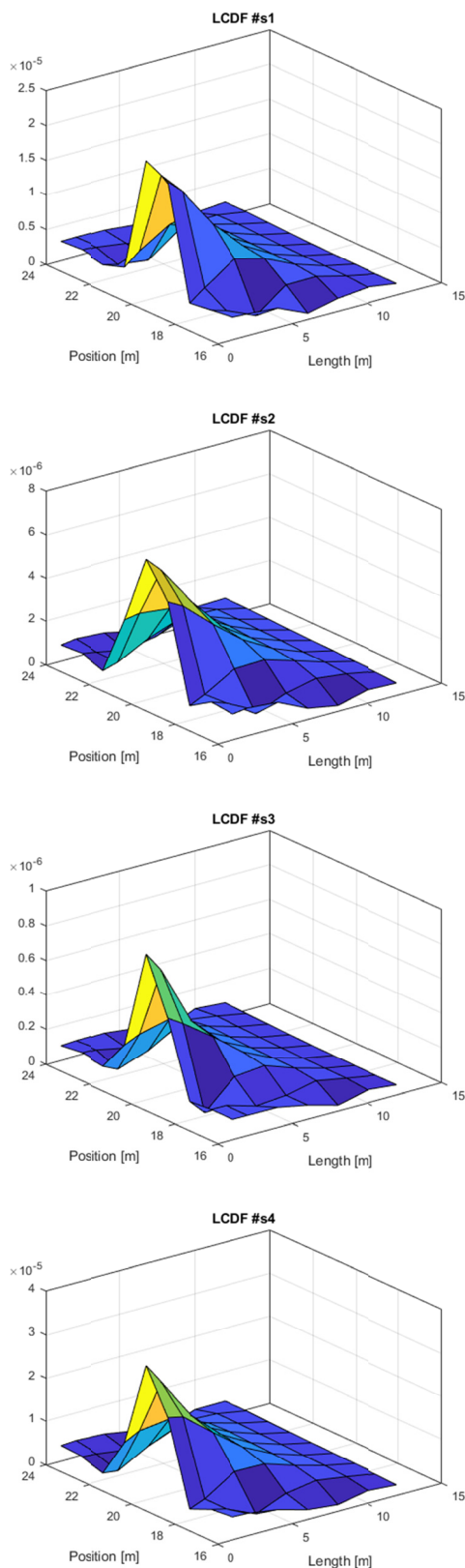


Figure 9. The LCDF index as a function of the position and the reference measurement length for each damage scenario.

REFERENCES

- Agarwal, S., Chaudhuri, S.R., 2015. Damage detection in large structures using mode shapes and its derivatives, *International Journal of Research in Engineering and Technology*, **4**, 80-87.
- Bartoli, G., Betti, M., Giordano, S., 2013. In situ static and dynamic investigations on the 'Torre Grossa' masonry tower, *Engineering Structures*, **52**, 718-733..
- Bartoli, G., Betti, M., Pintucchi, B., 2017a. Variation in modal properties of slender masonry structure due to damage. *Proceedings of the 2nd International Conference on Recent Advances in Nonlinear Models - Design and Rehabilitation of Structures. CoRASS 2017*. November 16-17, Coimbra, Portugal.
- Bartoli, G., Betti, M., Pintucchi, B., 2017b. Effects of damage on the dynamic modal properties of masonry towers. *Atti del XVII Congresso ANIDIS L'ingegneria sismica in Italia, ANIDIS 2017*. 17-21 settembre, Pistoia, Italia.
- Bartoli, G., Betti, M., Biagini, P., Borghini, A., Ciavattone, A., Girardi, M., Lancioni, G., Marra, A.M., Ortolani, B., Pintucchi, B., 2017c. Epistemic uncertainties in structural modelling: a blind benchmark for seismic assessment of slender masonry towers, *ASCE's Journal of Performance of Constructed Facilities*, **31**(5), 04017067.
- Betti, M., Facchini, L., Biagini, P., 2015. Damage detection on a three-storey steel frame using artificial neural networks and genetic algorithms, *Meccanica*, **50**(3), 875-886.
- Cavalagli, N., Comanducci, G., Ubertini, F., 2018. Earthquake-induced damage detection in a monumental masonry bell-tower using long-term dynamic monitoring data, *Journal of Earthquake Engineering*, **22**(1), 96-119.
- Ceravolo, R., Pistone, G., Zanotti Fragonara, L., Massetto, S., Abbiati, G., 2016. Vibration-based monitoring and diagnosis of cultural heritage: a methodological discussion in three examples, *International Journal Architectural Heritage*, **10**(4), 375-395.
- Chang, P.C., Flatau, A., Liu, S.C., 2003. Review paper: Health monitoring of civil infrastructure, *Structural Health Monitoring*, **2**(3), 257-267.
- Facchini, L., Betti, M., Biagini, P., 2014. Neural network based modal identification of structural systems through output-only measurement, *Computers and Structures*, **138**, 183-194.
- Frigui, F., Faye, J.P., Martin, C., Dalverny, O., Peres, F., Judenherc, S., 2018. Global methodology for damage detection and localization in civil engineering structures, *Engineering Structures*, **171**, 686-695
- Gentile, C., Guidobaldi, M., Saisi, A., 2016. One-year dynamic monitoring of a historic tower: damage detection under changing environment, *Meccanica*, **51**, 2873-2889.
- Lucchesi, M., Pintucchi, B., 2007. A numerical model for non-linear dynamics analysis of masonry slender structures, *European Journal of Mechanics A/Solids*, **26**, 88-105.



- Lucchesi, M., Pintucchi, B., Šilhavý, M., Zani, N., 2015. On the dynamics of viscous masonry beams, *Continuum Mechanics and Thermodynamics*, **27**, 349-365.
- Morassi, A., Vestroni, F. (Eds.), 2008. *Dynamic Methods for Damage Detection in Structures*, Springer-Verlag Wien.
- Pandey, A. K., Biswas, M., Samman, M.M., 1991. Damage detection from changes in curvature mode shapes, *Journal of Sound and Vibration*, **145**(2), 321-332.
- Pierdicca, A., Clementi, F., Isidori, D., Concettoni, E., Cristalli, C., Lenci, S., 2016. Numerical model upgrading of a historical masonry palace monitored with a wireless sensors network, *International Journal of Masonry Research and Innovation*, **1**, 74-99.
- Pintucchi, B., Zani, N., 2016. A simple model for performing nonlinear static and dynamic analyses of unreinforced and FRP-strengthened masonry arches, *European Journal of Mechanics A/Solids*, **59**, 210-231.
- Ramos, L.F., De Roeck, G., Lourenço, P.B., Campos-Costa, A., 2010. Damage identification on arched masonry structures using ambient and random impact vibrations, *Engineering Structures*, **32**, 146-162.
- Rucevskis, S., Wesolowski, M., 2010. Identification of damage in a beam structure by using mode shape curvature squares, *Shock and Vibration*, **17**, 601-610.
- Salawu, O.S., 1997. Detection of structural damage through changes in frequency: A review, *Engineering Structures*, **19**(9), 718-723.
- Sohn, H., Farrar, C.R., Hemez, F.M., Shunk, D.D., Stinemates, D.W., Nadler, B.R., 2003. A review of structural health monitoring literature: 1996-2001. *Los Alamos National Laboratory Report*, LA-13976-MS.
- Ubertini, F., Comanducci, G., Cavalagli, N., Pisello, A.L., Materazzi, A.L., Cotana, F., 2017. Environmental effects on natural frequencies of the San Pietro bell tower in Perugia, Italy, and their removal for structural performance assessment, *Mechanical Systems and Signal Processing*, **82**, 307-322.
- Wahab, M.M.A., De Roeck, G., 1999. Damage detection in bridges using modal curvatures: application to a real damage scenario, *Journal of Sound and Vibration*, **226**(2), 217-235.